Teagasc

AGRICULTURE AND FOOD DEVELOPMENT AUTHORITY

1

2 TITLE: Complexes between linoleate and native or aggregated β-lactoglobulin:

3 Interaction parameters and in vitro cytotoxic effect.

4 AUTHORS: Solène Le Maux, Saïd Bouhallab, Linda Giblin, André Brodkorb and

5 Thomas Croguennec

Complexes between linoleate and native or aggregated β-lactoglobulin: Interaction parameters and *in vitro* cytotoxic effect

Solène Le Maux[1,2,3], Saïd Bouhallab[1,2], Linda Giblin[3], André Brodkorb[3] and Thomas Croguennec[1,2,*]

[1] INRA, UMR1253 STLO, 65 rue de Saint Brieuc, F-35042 Rennes, France

[2] AGROCAMPUS OUEST, UMR1253 STLO, 65 rue de Saint Brieuc, F-35042 Rennes, France

[3] Teagasc Food Research Centre, Moorepark, Fermoy, Co. Cork, Ireland

[*] To whom correspondence should be addressed. Telephone: +33223485927. Fax: +0033223485350. E-mail: Thomas.Croguennec@agrocampus-ouest.fr

Authors e-mail address:

Solène Le Maux: Solene.Le.Maux@agrocampus-ouest.fr

Saïd Bouhallab: Said.Bouhallab@rennes.inra.fr

Linda Giblin: Linda.Giblin@teagasc.ie

André Brodkorb: Andre.Brodkorb@teagasc.ie

Thomas Croguennec: Thomas.Croguennec@agrocampus-ouest.fr

29

30 ***ABSTRACT***

31

32 The dairy protein β-lactoglobulin (βlg) is known to form complex with fatty acids (FA).

33 Because of industrial processing, βlg is often in non-native form in food products, which can

34 modify the FA/βlg complex properties. We investigated the interaction of bovine βlg in

35 selected structural forms (native βlg, covalent dimer and nanoparticles) with linoleate

36 (C18:2). Using fluorescence and Isothermal Titration Calorimetry, linoleate was found to bind

37 βlg in two types of binding sites. Regardless of the structural state of βlg, association

38 constants remained in the same order of magnitude. However, the stoichiometry increased up

39 to six fold for nanoparticles, compared to that of native βlg. The impact of these structural

40 changes on linoleate uptake *in vitro* was measured by cytotoxic assays on Caco-2 cells. The

41 order of cytotoxicity of linoleate was as follow: free>complexed to dimers>complexed to

42 nanoparticles>complexed to native βlg. Therefore, *in vitro* cytotoxicity of linoleate could be

43 modulated by altering the state of βlg aggregation, which in turn affects its binding capacity to

44 the FA.

45

46 **Key words**: β-lactoglobulin; Linoleate; Interaction; Aggregation; Cytotoxicity.

47

1   INTRODUCTION

β-lactoglobulin (βlg), the major whey protein in bovine milk, is present in a large number of food products. βlg is a member of lipocalin family, composed of 162 amino acids with a monomeric molecular weight of 18.4 kDa (Braunitzer, Chen, Schrank & Stangl, 1973). It contains nine β-strands labelled from A to I, and a three turns α-helices, that are arranged to form a globular protein structure (Creamer, Parry & Malcolm, 1983; Sawyer & Kontopidis, 2000). Eight antiparallel β-strands are organised in a β-barrel, shaped into a hydrophobic calyx. Under physiological conditions, native βlg exists in a non-covalent dimer/monomer equilibrium. However, βlg structure is highly sensitive to processing conditions used in food industries, especially the heat treatments that are applied during food manufacture to reach specific food textures or to reduce microbial load (Considine, Patel, Anema, Singh & Creamer, 2007; de Wit, 2009). Such treatments denature native βlg, leading to the formation of non-native monomers and aggregates of βlg in food products (de Wit, 2009).

βlg is able to bind small hydrophobic molecules such as fatty acids (FA) (Sawyer et al., 2000), and the formation of such complexes modifies FA digestion (Perez, Sanchez, Aranda, Ena, Oria & Calvo, 1992). It has been suggested that native βlg binds hydrophobic ligands in its internal calyx and on surface binding sites (Wu, Pérez, Puyol & Sawyer, 1999; Yang et al., 2008). However, FA binding to the βlg is sensitive to the physicochemical conditions of the medium. Several studies related the decrease of association constants between βlg and binding FA with a decrease in pH. Indeed, below pH 6.2, the calyx binding site is closed by the EF loop region, decreasing interaction with hydrophobic components (Ragona et al., 2000). Additionally, Wang, Allen, and Swaisgood (1998) demonstrated that a decrease in the proportion of native βlg dimer increased βlg affinity constant for palmitate. A number of

72 studies have assessed the interaction of ligands with heat treated βlg (O'Neill & Kinsella,

73 1988; Yang et al., 2008). However, these different studies have shown inconsistent changes in

74 the binding constants of such ligands with heat treated βlg compared to native form. This may

75 be due to the nature of the ligand, or to differences in the applied heat treatments (O'Neill et

76 al., 1988; Yang et al., 2008). In fact, aggregates differ in the parts of protein exposed and

77 therefore differ in how they react to heat (de Wit, 2009).

78 The essential long-chain fatty acid (LCFA) linoleic acid (LA, *cis,cis*-9,12-octadecadienoic

79 acid, n-6, 18:2) constitutes 1-3 % (w/w) of the total FA found in bovine milk fat (Jensen,

80 2002). LA serves as an essential precursor to a number of long chain metabolites (Mantzioris,

81 James, Gibson & Cleland, 1995; Russo, 2009). Its health benefits include anti-inflammatory

82 effects, improvements in serum lipoprotein profiles and reduction in the risk of cardiovascular

83 coronary artery disease (Zhao et al., 2005; Zock & Katan, 1998). Furthermore, LA, at high

84 concentrations, is cytotoxic to cancerous cells *in vitro* (Lu, He, Yu, Ma, Shen & Das, 2010).

85 However, bioaccessibility of FA is altered according to the structure of the food matrix (Le

86 Maux, Giblin, Croguennec, Bouhallab & Brodkorb, 2012; Mu, 2008; Singh, Ye & Horne,

87 2009). We previously demonstrated an interaction between the water soluble form of LA,

88 linoleate, and native βlg (Le Maux et al., 2012). This binding alters the cytotoxicity of

89 linoleate by decreasing its transport into the cell.

90 However, as βlg is often in non-native forms in food products, the aim of the present work

91 was to determine whether βlg structural forms alter the βlg/linoleate interaction and

92 consequently the linoleate cytotoxicity, indication of its transport into the cell. Therefore,

93 selected βlg aggregates of controlled size, covalent dimers and nanoparticles, were formed.

94 Binding properties of native βlg, covalent dimers and nanoparticles with linoleate were

95 measured by both isothermal titration calorimetry and intrinsic fluorescence. Cytotoxicity of

96 linoleate either free in solution or in complexes was measured for a better understanding of

97 the protein structure impacts on the FA transport.

98

99

100 *2   MATERIALS AND METHODS*

101

102   *Materials*

103

104   βlg (96 % purity) was obtained from Davisco Foods International, Inc. (Eden Prairie,

105 Minnesota) and sodium linoleate (purity $\geq$ 98 %) from Sigma-Aldrich (St. Louis, MO). All

106 other chemicals and solutions were purchased from Sigma-Aldrich unless stated otherwise.

107

108   ***Protein sample preparation and characterization***

109

110   *2.2.1   Formation of β-lactoglobulin dimers and nanoparticles*

111

112   Covalent dimers of βlg were formed using the protocol reported by Gulzar, Croguennec,

113 Jardin, Piot, and Bouhallab (2009). Briefly, βlg was dissolved in a 5 mM Bis-Tris buffer (pH

114 6.7), the final protein concentration was 5 g/L. Copper chloride ($CuCl_2$) was added to the βlg

115 solution at a Cu^{2+}/βlg molar ratio of 0.6. The solution was heated at 80°C for 30 min to form

116 covalent dimers, then cooled on ice. Covalent dimers were first dialyzed against 10 mM NaCl

117 (dialysis baths were changed every hour for 4 h) and then against distilled water for 48 h

118 (water bath was changed twice). Samples were then freeze-dried and stored at -20°C prior to

119 experiments.

120   Nanoparticles of βlg were formed according to the method of Schmitt et al. (2009)

121   Briefly, βlg was dissolved in Milli-Q water (Millipore, Carrigtwohill, Ireland), to a final

122   protein concentration of 10 g/L. The pH of the protein solution was adjusted to 5.9 using 1 M

123   HCl, before heating the solution at 85°C for 15 min, and then rapidly cooling on ice. Samples

124   were dialysed for 48 h against an excess of distilled water, freeze-dried and stored at -20°C

125   prior to experimental use.

126

127   *2.2.2   Characterization of native β-lactoglobulin, covalent dimers and nanoparticles*

128

129   <u>Quantification of β-lactoglobulin concentration in reconstituted solutions</u>

130   The concentration of native βlg and covalent dimers (expressed in monomer) were

131   determined by optical density using the extinction coefficient of βlg at 278 nm (ε_{278} = 0.96

132   L/g/cm).

133   For nanoparticles, the concentration of βlg monomers was quantified on a reduced sample

134   by the Bradford test following the manufacturer's instructions (Sigma-Aldrich). For

135   reduction, 470 µL of nanoparticle sample (1 mg of powder/mL) was dissolved in phosphate

136   buffered saline (PBS; 0.01 M phosphate buffer, 2.7 mM KCl, 137 mM NaCl, pH 7.4), 5 µL of

137   10 % SDS and 25 µL β-mercaptoethanol, and the mixture was heated at 95°C for 5 min.

138

139   <u>Characterisation of β-lactoglobulin samples using gel permeation-HPLC</u>

140   The proportion of monomers, dimers, oligomers and aggregates in βlg samples were

141   determined by gel permeation-HPLC (GP-HPLC) using a TSK G SW guard column (7.5 ×

142   7.5 mm, Tosoh Bioscience GmbH, Stuttgart, Germany) and a TSK G2000 SW column (7.5 ×

143   600 mm, Tosoh Bioscience GmbH) connected to an HPLC system, consisting of a Waters

144   2695 Separations Module (Waters, Milford, MA) and a Waters 2487 Dual λ Absorbance

145   Detector (Waters) working at 280 nm using Empower Pro software (Waters) to acquire and

146   analyse data. Solvent with 30 % (v/v) acetonitrile (LabScan Analytical Sciences, Dublin,

147   Ireland) and 0.1 % (w/v) trifluoracetic acid in Milli-Q water was used for protein elution at a

148   flow rate of 0.5 mL/min. The molecular-weight of the different molecular entities in the

149   samples was determined using a protein molecular-weight standard calibration set (Sigma-

150   Aldrich).

151   The molecular entities present in each βlg sample were determined as follows: solutions of

152   native βlg, covalent dimers and nanoparticles were prepared at 1 g/L in PBS. Nanoparticle

153   solutions were centrifuged at 12000 g in order to separate nanoparticles (pellet) from smaller

154   molecular entities (supernatant). Solutions of native βlg, covalent dimers and the supernatant

155   of nanoparticle solutions were filtered (0.22 µm filter) prior to injection onto GP-HPLC. The

156   proportions of monomers, dimers and higher size oligomers of βlg were determined from their

157   relative GP-HPLC chromatographic peak area obtained using Apex Track integration, and the

158   sample total chromatographic peak area. The proportion of monomers and aggregates in the

159   nanoparticle samples were determined from their chromatographic peak area in the

160   supernatant of the nanoparticle sample and the total chromatographic area of a solution of

161   native βlg prepared at 1 g/L. The proportion of the different molecular entities for each of the

162   βlg samples (native βlg, covalent dimers and nanoparticles) and of α-lactalbumin (αla,

163   impurity) were calculated. Native βlg sample contains 84.6 ± 1 % monomers, 5.4 ± 0.5 %

164   dimers, 5.4 ± 0.4 % oligomers and 4.6 ± 0.4 % of αla. Covalent dimers sample has 74.4 ± 3.1

165   % of dimers, 15.5 ± 1.4 % of residual monomers, 6.5 ± 1.6 % of oligomers and 3.6 ± 0.4 % of

166   αla. Nanoparticle sample has 77.6 ± 1.4 % of aggregates and 22.4 ± 1.4 % of monomers.

167

168   <u>Mean hydrodynamic diameter of nanoparticles</u>

169   To check the homogeneity of the preparation, the mean hydrodynamic diameter of the

170   aggregates in the nanoparticle sample was measured by dynamic light scattering using a

171   Zetasizer Nano ZS (Malvern Instruments Ltd., Malvern, Worcestershire, UK) equipped with a

172   4 mW helium/neon laser at a wavelength output of 633 nm. Particles sizing was performed at

173   25°C at 10 s intervals in a particle-sizing cell using backscattering technology at a detection

174   angle of 173°. Results were the mean of 13 runs. The intensity of light scattered from the

175   particles was used to calculate the mean hydrodynamic diameter (z-average mean), based on

176   the Stokes-Einstein equation, assuming the particles to be spherical. The mean hydrodynamic

177   diameter of aggregates (nanoparticles) was centered around 130 nm (data not shown).

178

179   *Linoleate/ β-lactoglobulin structure interaction*

180

181   *2.3.1   Isothermal titration calorimetry*

182

183   Isothermal titration calorimetry (ITC) was used to determine the interaction parameters

184   between the different forms of βlg and linoleate. ITC experiments were performed on a VP-

185   ITC microcalorimeter (Microcal, Northampton MA). Solutions of βlg (0.027 mM) and

186   linoleate (1.65 mM) in PBS were degassed under vacuum before titration experiments. The

187   reference cell was filled with PBS, and the sample cell (1.425 mL) was filled with βlg

188   solution. βlg was titrated at 25°C with 29 successive linoleate injections of 10 µL. The

189   injection time was 20 s, and the time between injections was fixed at 600 s to achieve

190   thermodynamic equilibrium. During titrations, the solution in the sample cell was stirred at

191   310 rpm to ensure complete mixing. The control measurement was obtained by titrating

192   sodium linoleate into PBS buffer using the same injection procedure. The control

193   measurement was subtracted from the βlg titration with linoleate and the first injection peak

194   was systematically ignored for the data analysis. Data were analysed using MicroCal ORIGIN

195   version 7.0 (Microcal). The integrated area of each peak was plotted versus the linoleate/βlg

196   monomer molar ratio. The "two sets of binding sites" model was the best fit for all

197   experiments, providing the binding parameters K_{a1}, K_{a2}, n_1, and n_2 (K_a and n are the

198   association constant and the stoichiometry, respectively). Each measurement was performed

199   in triplicate.

200

201   *2.3.2   Intrinsic fluorescence*

202

203   Intrinsic fluorescence spectra were recorded at 345 nm using an excitation wavelength of

204   278 nm. For each titration, a fluorescence spectrum was recorded from 300 to 450 nm in order

205   to observe deviation in fluorescence properties of the protein. Experiments were performed at

206   25°C on a SPEX 112 spectrofluorometer (Jobin-Yvon, Longjumeau, France), using 10×10

207   mm quartz cuvette. Excitation and emission slits were both set to 5 nm. βlg solutions in PBS

208   (3 mL at 10 µM) were titrated with successive 3 µL injections of 5 mM linoleate, upto a

209   linoleate/βlg molar ratio of 10. The solution was agitated by pipetting up and down several

210   times and a 5 min equilibrium time was respected prior to each measurement. An N-acetyl-

211   tryptophanamide (NATA) blank was titrated following the same procedure in order to

212   subtract the inner filter effect caused by the FA. NATA fluoresces similarly to tryptophan but

213   does not bind FA (Cogan, Kopelman, Mokady & Shinitzky, 1976). The concentration of

214   NATA was chosen to have the same initial fluorescence (without FA) as the fluorescence of

215   βlg solutions. Fluorescence of NATA was subtracted from fluorescence intensity

216   measurements of the ligand/protein complexes for all the linoleate/βlg molar ratios tested.

217   Each measurement was performed in triplicate. Fluorescence data were fitted using two

218   different methods.

219   In method 1, L_{free}, L_{total} and L_{bound} represent the concentration of free, total and bound

220   linoleate, respectively, P_{total} is the concentration of βlg, ν is the fraction of linoleate molecules

221   bound per mole of protein (ν varies from 0 to n), n the number of linoleate bound to βlg at

222   saturation (number of sites), and f_i the fraction of one site of the protein to be occupied by a

223   ligand (f_i varies from 0 to 1). Then:

224    $$L_{total} = L_{free} + L_{bound} \quad (1)$$

225    $$\nu = \frac{L_{bound}}{P_{total}} = nf_i \quad (2)$$

226   Combining equations (1) and (2) we deduce that:

227    $$L_{total} = L_{free} + nP_{total}f_i \quad (3)$$

228   The value of fi is determined using the initial fluorescence intensity (F_0), the fluorescence

229   intensity at saturation (F_{max}) and the fluorescence intensity at the ratio ligand/protein i (F_i) as

230   indicated in equation (4):

231    $$f_i = \frac{F_i - F_0}{F_{max} - F_0} \quad (4)$$

232   When F_{max} was not reached experimentally, it was determinated by fitting using an

233   exponential phase decay model on Graph-Pad Prism software. The value of n was determined

234   by plotting L_{total} in function of $P_{total}f_i$. The data were fitted using a sequential linear regression

235   in Graph-Pad Prism software 3.03 (GraphPad Software Inc., La Jolla CA).

236   Method 2 is an adaptation of the Scatchard plot. In the Scatchard plot described below, K_a

237   is the association constant:

238    $$\frac{\nu}{L_{free}} = nK_a - \nu K_a \quad (5)$$

239   Equations (3) and (5) can be rearranged as: $P_{total}\left(1 - f_i\right) = \frac{L_{total}}{n}\left(\frac{1}{f_i} - 1\right) - \frac{1}{nK_a} \quad (6)$

240   By fitting this equation using Graph-Pad Prism software, n and K_a were determined.

241

Preparation of linoleate/β-lactoglobulin complexes for biological assay

2.4.1   Preparation of complexes

Linoleate/βlg complexes were prepared by mixing βlg samples with sodium linoleate according to Lišková et al. (2011) with modifications as described in Le Maux et al. (2012). Briefly, 0.163 mM βlg, in its native form, covalent dimers or nanoparticles, were dissolved in PBS, and sodium linoleate was added to reach final linoleate/βlg molar ratios of 5, 7.5 or 10. Solutions containing native βlg were heated at 60°C for 30 min to facilitate βlg/linoleate interaction and rapidly cooled on ice. Solutions containing covalent dimers or nanoparticles were mixed overnight at room temperature. Samples were dialysed against distilled water for 72 h with dialysis bags of nominal cut-off of 3500 Da. Samples were freeze-dried and powders stored at -20°C prior to experiments.

2.4.2   Determination of fatty acid content by gas chromatography

The FA content of the complexes was determined by gas chromatography (GC) following a protocol adapted from Palmquist and Jenkins (2003) and Coakley, Ross, Nordgren, Fitzgerald, Devery, and Stanton (2003) and described in detail previously (Le Maux et al., 2012). Briefly, the internal standard tridecanoic acid (C13:0) was added to ~4 mg of complexes. FA were converted to fatty acid methyl esters (FAME) and were analysed using a CP-SELECT CB column for FAME (100 m, 0.25 mm, 0,25 μm film thickness, Varian BV, Middelburg, the Netherlands), adapted on a Varian 3400 GLC (Varian, Walnut Creek, CA) connected to a flame ionization detector.

266

267   *2.4.3   Complexes analysis by polyacrylamide gel electrophoresis*

268

269   Samples were analysed by sodium dodecyl sulphate polyacrylamide gel electrophoresis

270   (SDS-PAGE). Mini-PROTEAN TGX precast Gels (4-20 % resolving gel, Bio-Rad

271   Laboratories Inc., Hercules, CA) were used on a Mini Protean II system (Bio-Rad) according

272   to the manufacturer's instructions. Samples were prepared under non-reducing (in the absence

273   of β-mercaptoethanol) and reducing (in the presence β-mercaptoethanol) conditions. Protein

274   was visualized by staining with Coomassie blue (Bio-Safe Coomassie Stain G-250, Bio-Rad).

275   An Amersham Low Molecular Weight Calibration kit (14.4 to 97 kg/mol, GE Healthcare UK

276   Limited, UK) was used as molecular weight standards.

277

278   **Cell Culture and cytotoxicity assay**

279

280   The Caco-2 cell line was purchased from the European Collection of Cell Cultures

281   (collection reference: ECACC 86010202). It was derived from human colonic

282   adenocarcinoma cells and can mimic the enterocytes of the intestine.

283   Cells cultures were maintained in a humidified 37°C incubator with a 5 % CO_2 in air

284   atmosphere. Cells were routinely grown in 75 cm^2 plastic flasks in Dulbecco's modified Eagle

285   medium (DMEM) containing 4.5 g/L glucose and 0.584 g/L L-glutamine. Media for

286   subculture was supplemented with 10 % (v/v) foetal bovine serum (FBS), 100 U/mL

287   penicillin and 100 mg/mL streptomycin. At 80 % confluency, cells were trypsinised with 0.25

288   % trypsin/EDTA, diluted 1:6 in media and reseeded. The growth medium was changed three

289   times a week. All cells used in these studies were between passage number 20 and 31.

290   Cytotoxicity of test samples on Caco-2 cell proliferation was determined by MTS assay,

291   using CellTiter 96 Aqueous One Solution Cell Proliferation Assay according to the

292   manufacturer's instructions (Promega Corporation, Madison, Wisconsin) and previously

293   described in Le Maux et al. (2012). Briefly, 96-well plates were seeded with 2×10^4 Caco-2

294   cells/well, using serum-free media. After 24 h, cells were treated with different concentrations

295   of linoleate (0 to 200 μM) or linoleate/βlg complexes (higher linoleate/βlg complex which

296   contained 0 to 200 μM linoleate as determined by GC) in serum-free media for 24 h. After the

297   use of One Solution Cell Proliferation reagent, viability was defined as the ratio of absorbance

298   of treated cells to untreated cells (cells exposed to serum-free Media only) at 490 nm. Cells

299   exposed to the different controls of βlg were subtracted to the corresponding samples. Each

300   cell exposure was performed in triplicate.

301   The Lethal Dose 50 (LD_{50}) values, the concentration required to decrease the cell viability

302   by 50 %, were determined using Graph-Pad Prism software 3.03 (GraphPad). The sigmoidal

303   dose-response with variable slope was used to fit the measured curves and calculate LD_{50}.

304

305   *Statistical analysis*

306

307   Where appropriate, results were statistically analysed using the R software package

308   version 2.15.1 (R Foundation for Statistical Computing, Vienna, Austria) and the ANOVA

309   system with a Tukey's least significant difference comparison. *P*-Values less than 0.05 were

310   deemed to be statistically significant.

311

312

313   *3   RESULTS*

314

315   ***Binding properties of the different β-lactoglobulin forms with linoleate***

316

317   Binding parameters, determined at 25°C using ITC and intrinsic fluorescence

318   spectroscopy, were expressed on the basis of βlg monomeric units.

319   ITC data revealed an exothermic signal for the interaction between linoleate and all the

320   βlg forms tested. Increasing the amount of linoleate in the titration cell resulted in a

321   progressive decrease of the exothermic signal due to the saturation of the binding sites (Figure

322   1A). Regardless of the states of βlg aggregation, the data were best fitted with a two sets of

323   binding sites model. The number of binding sites for each set of binding sites (n) and the

324   corresponding association constant (K_a) could be determined from the fitted curves (Table 1).

325   Similar association constants were observed for all βlg forms for each set of binding sites. The

326   K_a values for the first and second sets of binding sites were close to 10^6 M^{-1} and 10^4 M^{-1},

327   respectively. Molar ratio of linoleate bound to βlg monomer (n) varied for the first set of

328   binding sites between 0.53 ± 0.08 for covalent dimers and 0.92 ± 0.29 for nanoparticles. For

329   the second set of binding sites, n varied somewhat more: native βlg (6.79 ± 0.05), covalent

330   dimers (8.64 ± 0.54) and nanoparticles (10.25 ± 1.64).

331

332   Intrinsic fluorescence titration is based on the change in the intensity of βlg tryptophan

333   fluorescence. The maximum emission wavelength was 345 nm, 353 nm and 350 nm for native

334   βlg, covalent dimers and nanoparticles, respectively; therefore aggregated βlg caused a red

335   shift. However, the fluorescence spectra had a similar shape for all the βlg forms tested and

336   the changes in fluorescence intensity consecutive to linoleate addition were correlated at the

337   three wavelengths. Therefore the fluorescence changes were followed at 345 nm, which is the

338   wavelength of maximal fluorescence intensity of native protein. In the titration range used in

339   this study, the change in fluorescence intensity reached a maximum of 10.5 ± 1.3 %, $21.7 \pm$

340   1.6 % and 32.2 ± 2.1 % from the initial fluorescence intensity for native βlg, covalent dimers

341   and nanoparticles, respectively (Figure 1B). Increasing the linoleate concentration in native

342   βlg samples induced an increase in fluorescence intensity at 345 nm. This increase levels off

343   when the linoleate/βlg molar ratio reaches 3. In contrast, the fluorescence intensity of the

344   covalent dimers and of the nanoparticles decreased continuously up to a linoleate/βlg molar

345   ratio of 10. For each titration, fluorescence data were fitted with two different models.

346   In the first model the total concentration of linoleate is plotted as a function of total

347   concentration of protein and variation in fluorescence intensity ($P_{total}.f_i$). It gave access to the

348   number of binding sites (n), which are determined from the slope of the graphical

349   representation. For the entire titration, the graphical representation can be fitted with two

350   straight lines, indicating the presence of two sets of binding sites (Table 1). The number of

351   binding sites varied according to the βlg forms. From linoleate/native βlg to

352   linoleate/nanoparticles complexes, n_1 increased from 2.38 ± 0.12 to 15.74 ±0.55 and n_2 from

353   6.02 ± 0.29 to 40.73 ± 2.17.

354   The second model was an adaptation of the Scatchard plot, in which the maximum

355   fluorescence (F_{max}) was required for the plot construction. However, F_{max} was not reached

356   with a 10 linoleate/βlg molar ratio for the complexes made with the covalent dimers and the

357   nanoparticles. Therefore, the fit of the Scatchard plot was obtained using the experimental

358   F_{max} only for the complex made of linoleate and native βlg. An extrapolated F_{max} was used for

359   the Scatchard plot of the linoleate/covalent dimers complex (Table 1). Unfortunately, the

360   fluorescence data for the linoleate/nanoparticles complexes could not be fitted correctly using

361   extrapolated F_{max}. The thermodynamic constants (K_a) for the two sets of binding sites were

362    $9.20 ± 2.65 × 10^5$ M^{-1} and $0.62 ± 0.49 × 10^5$ M^{-1} for the linoleate/native βlg complex and

363    $14.67 ± 2.12 × 10^5$ M^{-1} and $0.37 ± 0.13 × 10^5$ M^{-1} for the linoleate/covalent dimers complex.

364   These values of association constants were in the same range than those deduced from ITC

365   data. The stoichiometry n_1 was 2.45 ± 0.07 and 10.31 ± 0.05 while n_2 was 5.27 ± 1.5 and

366   15.29 ± 0.71 for linoleate/native βlg and linoleate/covalent dimers complexes respectively.

367

368   ***Changes in the structure of the linoleate/β-lactoglobulin complexes***

369

370   Complexes of linoleate with native βlg, covalent dimers and nanoparticles were analysed

371   by SDS-PAGE and GP-HPLC in order to identify changes in the aggregation state of βlg

372   following linoleate interaction. Previously we demonstrated that native βlg aggregated into

373   dimers and oligomers in the presence of linoleate (Le Maux et al., 2012). Figure 2A confirms

374   this observation with SDS-PAGE analysis of native βlg, under non-reducing conditions,

375   showing a major band corresponding to the βlg monomer with small amount of dimers and

376   trimers. The presence of linoleate increases the amount of βlg dimers and oligomers at the

377   expense of βlg monomers. In contrast, the presence of linoleate had almost no effect on

378   covalent dimers except a slight decrease in the intensity of the residual βlg monomer band

379   (Figure 2B). A similar result is obtained for the SDS-PAGE of the complexes made with

380   nanoparticles (Figure 2C). In this latter case, nanoparticles did not enter the separation gel

381   because of their high size. Under reducing conditions, SDS-PAGE for all the complexes and

382   the βlg controls (without linoleate) were similar. Figure 2D is a representation of these results

383   depicting nanoparticles and linoleate/nanoparticles complexes prepared at three different

384   linoleate/βlg molar ratio (5, 7.5 or 10), under reducing conditions. Taking the non-reducing

385   and reducing results together, linoleate induced aggregation of βlg stabilised by

386   intermolecular disulphide bonds.

387

388   GP-HPLC chromatograms of complexes formed with native βlg, covalent dimers and

389   nanoparticles were integrated and the proportion of βlg monomers, dimers and oligomers

390　(trimers and tetramers) as a function of the initial linoleate/βlg molar ratio are shown in Table

391　2. A decrease in the concentration of monomers in the presence of linoleate were observed for

392　all the βlg forms, in agreements with the SDS-PAGE experiments. The monomeric proportion

393　decreased from 88.5 ± 5.2 % to 51.1 ± 4.9 % using native βlg, from 16.3 ± 1.5 % to 13.4 ± 0.6

394　% for complexes using covalent dimers and from 22.4 ± 1.4 % to 10.6 ± 1.9 %, for complexes

395　using nanoparticles with an initial molar ratio of linoleate/βlg varying from 0 to 10.

396　Concomitantly, an increase of the protein aggregation was also observed. As predicted the

397　difference in aggregation by increasing the linoleate/βlg molar ratio was more pronounced for

398　native βlg than the other forms of βlg assayed.

399

400　　　　　　*Cytotoxicity of linoleate bound to the different forms of β-lactoglobulin*

401

402　　　　The effect of linoleate (0 to 200 µM), bound to the different forms of βlg, on Caco-2 cell

403　viability was measured. For quantifying the effect of the bound linoleate only, the complexes

404　were dialysed to remove unbound linoleate. After dialysis, the exact stoichiometry of

405　linoleate/βlg complexes was determined from freeze-dried complexes using GC (Figure 3).

406　The amount of linoleate bound to βlg increased when the initial linoleate/βlg molar ratio was

407　increased. This increase varied depending on the βlg form with more linoleate binding

408　increasing in the order of nanoparticles > covalent dimers > native βlg. Only the complexes

409　prepared with the higher linoleate/βlg molar ratio were used for cytotoxicity experiments

410　(Figure 4). No cytotoxic effect was detected for any of the βlg forms used at the

411　concentrations assayed when employed in the absence of linoleate (data not shown). Free

412　linoleate has a LD_{50} of 58.0 ± 4.2 µM (Le Maux et al., 2012). Comparatively, the LD_{50} of the

413　complexes were all significantly different ($p<0.001$). The linoleate/native βlg complex was

414　not cytotoxic to Caco2 cells at the concentrations tested ($LD_{50} \gg 200$ µM complex). LD_{50}

415   was 80.0 ± 3.1 μM for linoleate/covalent dimers complex, and 189.0 ± 4.1 μM for

416   linoleate/nanoparticles complex.

417

418

419   *4   DISCUSSION*

420

421   The structural state of βlg modified its binding properties to linoleate. This was

422   demonstrated using βlg intrinsic fluorescence and ITC measurements albeit the determined

423   stoichiometry of the two techniques differed slightly. The number of binding sites determined

424   from ITC data for the interaction between linoleate and native βlg showed lower n_1 value, but

425   a higher n_2 value compared to those deduced from intrinsic fluorescence data. However, the

426   total number of binding sites ($n_1 + n_2$) for linoleate to native βlg was similar (around 7.5 to 8

427   linoleate bound to the βlg native protein) regardless of technique and method used for data

428   fitting. The binding parameters from βlg intrinsic fluorescence titration gave a higher number

429   of binding sites for linoleate to covalent dimers and to nanoparticles than the ITC data. This

430   discrepancy may have resulted from (i) the intrinsic fluorescence data that cumulates inner

431   filter and non-specific quenching of the fluorescence spectrum of the complex under study

432   and/or (ii) the ITC signal complexity that includes all energetic changes occurring during the

433   titration such as structural changes of protein, modifications to protein and/or ligand hydration

434   (Bouchemal, 2008). Similarly, Loch et al. (2012a) found a stoichiometry lower than 1 mole

435   for lauric and myristic acids per mole of βlg when the interaction was studied by ITC while

436   one FA was found in the calyx of native βlg by Xray crystallography with resolution 1.9-2.1

437   Å. According to these authors, this may be related to the weak interaction between the FA and

438   βlg. Spector and Fletcher (1970) demonstrated that stearic acid exhibited a secondary set of

439   binding sites to βlg with the number of sites varying from 2 to 24, using the same set of data

440   analyzed with different fitting parameters.

441   Comparative analysis of the fluorescence data show differences in the fluorescence

442   changes for the native βlg experiments relative to the aggregated βlg experiments. The

443   intrinsic fluorescence of covalent dimers and nanoparticles decreased the titration of linoleate

444   due to tryptophan quenching by the FA. Conversely, the intrinsic fluorescence of native βlg

445   increased in the presence of linoleate. This can be explained by the compensation of the

446   tryptophan quenching effect by the denaturation of the protein caused by the binding with

447   linoleate, which reduced the tryptophan quantification by Cys-Cys disulphide bonds (Renard,

448   Lefebvre, Griffin & Griffin, 1998).

449

450   The number of linoleate bound per βlg molecule increased with the degree of

451   aggregation (native βlg < covalent dimers < nanoparticles) but the association constants for

452   each sets of binding sites remained similar. Several studies have demonstrated the impact of

453   βlg denaturation/aggregation for ligand binding, but were dependent on the type of ligands

454   and/or the structure of the aggregates (Ron, Zimet, Bargarum & Livney, 2010; Shpigelman,

455   Israeli & Livney, 2010). Hydrophobic ligands are able to bind native βlg on hydrophobic

456   patches of the protein surface and in the internal calyx if specific structural properties of the

457   ligands are respected (Kontopidis, Holt & Sawyer, 2004). The changes in binding parameters

458   are related to the structural changes of βlg, which occur during heat denaturation/aggregation

459   (de Wit, 2009). Heat-induced protein unfolding exposes internal hydrophobic patches(de Wit,

460   2009) that constitute additional potential binding sites for hydrophobic ligands. Even if they

461   are usually of low specificity and low affinity, these hydrophobic patches could be

462   responsible for the higher ratio of linoleate bound per βlg molecule in the covalent dimers and

463   nanoparticles compared to the native form of βlg. The higher degree of aggregation in the

464   nanoparticles, compared to covalent dimers, could also create hydrophobic pockets, trapping

465   more ligands with weak affinity. Indeed, nanoparticles are microgels, which have more

466   hydrophobic binding sites available compared to native βlg as shown by anilino naphthalene

467   sulfonic acid (ANS) fluorescence (Schmitt et al., 2009). In addition, the internal calyx of βlg

468   is modified during the heat-denaturation and aggregation of βlg. Consequently the specific

469   affinity to the ligand at this site could be affected. The formation of covalent dimers involves

470   the displacement of the free Cys121 that potentially distorts the calyx, decreasing its affinity

471   for linoleate. O'Neill et al. (1988) showed that heat-denaturation of βlg (75°C up to 20 min)

472   increased the number of binding sites for 2-nonanone but decreased its association constant.

473   Yang, Chen, Chen, Wu, and Mao (2009) found a weaker binding, with a lower n, when

474   vitamin D3 was bound to heat denatured βlg (100°C for 16 min) compared to native βlg.

475   Similar conclusions were reported by Spector et al. (1970) who found lower binding constants

476   between palmitate and βlg when the protein was heat treated from 55 to 80°C. These different

477   ligands were shown to specifically interact in the calyx of βlg that is affected by the βlg

478   denaturation. Unlike these studies, conformational changes of βlg do not lead to a change in

479   the affinity for linoleate at the first set of binding sites. This is rather surprising, since the

480   central cavity contains the binding site with strongest affinity for linoleate, as shown by 2.1 Å

481   resolution crystallography (PBD ID: 4DQ4, Loch et al. (2012b)). However, it is possible that

482   some specific protein structures are selected for crystal formation leading to different results

483   when protein in solid or liquid states are compared.

484

485   Cytotoxic assays represent an excellent method for determining changes in the

486   bioaccessibility of FA to Caco-2 cells since the linoleate must enter cells to be cytotoxic (Lu

487   et al., 2010). In the present study, exposure of the cells to linoleate/βlg complexes resulted in

488   a decrease in cytotoxicity compared to free linoleate. Therefore, we can postulate that binding

489   of linoleate to all the βlg forms decreased the bioaccessibility of the FA. After a 24 h exposure

490   period, linoleate bound to βlg nanoparticles had a higher cytotoxic effect compared to

491   linoleate bound to native βlg. This could be explained by the higher binding capacity of

492   nanoparticles for the FA compared to native βlg:8.9 linoleate per βlg nanoparticles versus 3.3

493   linoleate per native βlg. As only 0.6 or 0.9 linoleate is strongly bound per 1 βlg molecule in

494   the nanoparticular or native state, respectively (ITC data), the fraction of linoleate bound with

495   a lower affinity is much higher for the nanoparticles. This may explain the higher

496   bioaccessibility of linoleate when bound to the nanoparticles. Spector et al. (1970)

497   demonstrated that palmitate bound to βlg was taken up faster by Ehrlich ascites tumor cells

498   compared to palmitate bound to bovine albumin because palmitate binds to bovine albumin

499   with a higher affinity than to βlg. Consequently, the FA was more bioaccessible to the cells

500   when bound to βlg than to bovine albumin. Interestingly, linoleate/covalent dimer complexes

501   were more cytotoxic than linoleate/nanoparticles complexes, even though the amount of

502   linoleate bound with higher K_a was similar, as determined by ITC. As native βlg protects the

503   cells against the linoleate cytotoxicity, this difference in cell viability may be the result of the

504   different proportions of βlg monomers present in the test samples (22.4 % βlg monomers in

505   the nanoparticle sample compared to 16.3 % βlg monomers in the covalent dimer sample,

506   prior to the addition of linoleate). In addition, to obtain the same linoleate concentration, a

507   higher quantity of complex was needed for the linoleate/covalent dimers complex. The molar

508   ratios were 8.9 linoleate per βlg in the nanoparticles versus 4.0 linoleate per βlg in covalent

509   dimers. However, we have previously demonstrated that increasing βlg concentration

510   increased the linoleate uptake by Caco-2 cells even if the kinetic of transport is slower than

511   free linoleate (Data not shown). Other studies have reported the opposite effect, with the

512   binding of a given ligand to βlg increasing the ligand bioaccessibility. Indeed, Yang et al.

513   (2009) observed that vitamin D_3, which is practically insoluble in water, was transported more

514   effectively bound to βlg than free vitamin D₃ in a mouse model. Proteins may affect

515   differently the bioaccessibility of the ligand in function of the ligand solubility. The potential

516   contribution of residual copper used to prepare βlg covalent dimer in the cytotoxic effect of

517   this oligomer cannot be excluded. Copper by itself at concentrations up to 5 mg/L was not

518   cytotoxic (data not shown). However, copper was reported to be a potent catalyst of FA

519   oxidation (Frémont, Belguendouz & Delpal, 1999; Kleinveld, Hak-Lemmers, Stalenhoef &

520   Demacker, 1992). Peroxidated FA are reported to be more cytotoxic than FA (Alghazeer, Gao

521   & Howell, 2008). Hence, the occurrence of a peroxidated form of linoleate which would

522   increase its cytotoxicity cannot be ruled out.

523

524   This study has demonstrated that linoleate can bind to different structural states of βlg

525   (native, covalent dimers, nanoparticles). Binding capacity but not affinity was affected by the

526   protein structure. Stoichiometries increased with the size of the protein aggregates. This is

527   probably due to the exposure of hydrophobic sites during the protein denaturation and the

528   formation of hydrophobic pockets at the surface or in the inner structure of the aggregates.

529   Changes in the binding properties modified the cytotoxicity of the complexes. Consequently,

530   it is proposed that the *in vitro* bioaccessibility of linoleate can be modulated by changing

531   protein structures, which subsequently modifies the ligand binding parameters. This could be

532   of interest in relation to optimizing the design of food products from a sanitary, textural and

533   health benefit perspective. From a nutritional point of view, one question that arises is how

534   these various protein/FA complexes react to digestive enzymes. Studies are in progress to

535   determine the behaviour of complexes under simulated gastro-intestinal *in vitro* digestion and

536   the subsequent effect of digestion on FA cytotoxicity and uptake.

537

538

5   *ABBREVIATIONS*

αla, α-lactalbumin; βlg, β-lactoglobulin; CLA, conjugated linoleic acid; CMC, critical micelle concentration; DMEM, Dulbecco's modified Eagle medium; FA, fatty acid; FAME, fatty acid methyl ester; FBS, foetal bovine serum; GC, gas chromatography; GP-HPLC, gel permeation high performance liquid chromatography; ITC, isothermal titration calorimetry; K_a, association constant; LA, linoleic acid; LCFA, long chain fatty acid; n, reaction stoichiometry; NATA, N-acetyl-tryptophanamide, PBS, phosphate buffered saline;

6   *ACKNOWLEDGEMENTS*

7   *REFERENCES*

Alghazeer, R., Gao, H. L., & Howell, N. K. (2008). Cytotoxicity of oxidised lipids in cultured colonal human intestinal cancer cells (caco-2 cells). *Toxicology Letters, 180*(3), 202-211.

Bouchemal, K. (2008). New challenges for pharmaceutical formulations and drug delivery systems characterization using isothermal titration calorimetry. *Drug discovery today, 13*(21-22), 960-972.

Braunitzer, G., Chen, R., Schrank, B., & Stangl, A. (1973). Die sequenzanalyse des β-lactoglobulins. *Hoppe-Seyler´ s Zeitschrift für physiologische Chemie, 354*(2), 867-878.

Coakley, M., Ross, R. P., Nordgren, M., Fitzgerald, G., Devery, R., & Stanton, C. (2003). Conjugated linoleic acid biosynthesis by human-derived Bifidobacterium species. *Journal of Applied Microbiology, 94*(1), 138-145.

Cogan, U., Kopelman, M., Mokady, S., & Shinitzky, M. (1976). Binding affinities of retinol and related compounds to retinol binding proteins. *European Journal of Biochemistry, 65*(1), 71-78.

Considine, T., Patel, H. A., Anema, S. G., Singh, H., & Creamer, L. K. (2007). Interactions of milk proteins during heat and high hydrostatic pressure treatments - A review. *Innovative Food Science & Emerging Technologies, 8*(1), 1-23.

Creamer, L. K., Parry, D. A. D., & Malcolm, G. N. (1983). Secondary structure of bovine beta-lactoglobulin B. *Archives of Biochemistry and Biophysics, 227*(1), 98-105.

de Wit, J. N. (2009). Thermal behaviour of bovine beta-lactoglobulin at temperatures up to 150 degrees C. a review. *Trends in Food Science & Technology, 20*(1), 27-34.

Frémont, L., Belguendouz, L., & Delpal, S. (1999). Antioxidant activity of resveratrol and alcohol-free wine polyphenols related to LDL oxidation and polyunsaturated fatty acids. *Life Sciences, 64*(26), 2511-2521.

Gulzar, M., Croguennec, T., Jardin, J., Piot, M., & Bouhallab, S. (2009). Copper modulates the heat-induced sulfhydryl/disulfide interchange reactions of beta-Lactoglobulin. *Food Chemistry, 116*(4), 884-891.

Jensen, R. G. (2002). The composition of bovine milk lipids: January 1995 to December 2000. *Journal of Dairy Science, 85*(2), 295-350.

Kleinveld, H. A., Hak-Lemmers, H., Stalenhoef, A., & Demacker, P. (1992). Improved measurement of low-density-lipoprotein susceptibility to copper-induced oxidation: Application of a short procedure for isolating low-density lipoprotein. *Clinical Chemistry, 38*(10), 2066-2072.

Kontopidis, G., Holt, C., & Sawyer, L. (2004). Invited review: Beta-lactoglobulin: Binding properties, structure, and function. *Journal of Dairy Science, 87*(4), 785-796.

Le Maux, S., Giblin, L., Croguennec, T., Bouhallab, S., & Brodkorb, A. (2012). Beta-lactoglobulin as a molecular carrier of linoleate: Characterisation and effects on intestinal epithelial cells in vitro. *Journal of Agricultural and Food Chemistry, 60*(37), 9476–9483.

Lišková, K., Auty, M. A. E., Chaurin, V., Min, S., Mok, K. H., O'Brien, N., Kelly, A. L., & Brodkorb, A. (2011). Cytotoxic complexes of sodium oleate with beta-lactoglobulin. *European Journal of Lipid Science and Technology*, 1207-1218.

Loch, J., Polit, A., Bonarek, P., Olszewska, D., Kurpiewska, K., Dziedzicka-Wasylewska, M., & Lewiński, K. (2012a). Structural and thermodynamic studies of binding saturated fatty acids to bovine beta-lactoglobulin. *International Journal of Biological Macromolecules, 50*(4), 1095-1102.

Loch, J., Polit, A., Bonarek, P., Ries, D., Kurpiewska, K., Dziedzicka Wasylewska, M., & Lewi ski, K. (2012b). Bovine beta-lactoglobulin complex with linoleic acid. In *URL (www.rcsb.org/pdb/explore/explore.do?structureId=4DQ4) DOI:10.2210/pdb4dq4/pdb*, vol. (most recent access 5 June 2012)).

Lu, X., He, G., Yu, H., Ma, Q., Shen, S., & Das, U. N. (2010). Colorectal cancer cell growth inhibition by linoleic acid is related to fatty acid composition changes. *Journal of Zhejiang University-Science B, 11*(12), 923-930.

Mantzioris, E., James, M. J., Gibson, R. A., & Cleland, L. G. (1995). Differences exist in the relationships between dietary linoleic and alpha-linoleic acids and their respective long-chain metabolites. *American Journal of Clinical Nutrition, 61*(2), 320-324.

Mu, H. (2008). Bioavailability of omega-3 long-chain polyunsaturated fatty acids from foods. *Agro Food Industry Hi-Tech: Focus on Omega-3, 19*(4), 24-26.

618 O'Neill, T., & Kinsella, J. (1988). Effect of heat treatment and modification on conformation
619 and flavor binding by beta-lactoglobulin. *Journal of Food Science, 53*(3), 906-909.
620 Palmquist, D. L., & Jenkins, T. C. (2003). Challenges with fats and fatty acid methods.
621 *Journal of Animal Science, 81*(12), 3250-3254.
622 Perez, M. D., Sanchez, L., Aranda, P., Ena, J., Oria, R., & Calvo, M. (1992). Effect of beta-
623 lactoglobulin on the activity of pregastric lipase. A possible role for this protein in
624 ruminant milk. *Biochimica et Biophysica Acta (BBA) - Lipids and Lipid Metabolism,*
625 *1123*(2), 151-155.
626 Ragona, L., Zetta, L., Fogolari, F., Molinari, H., Pérez, D. M., Puyol, P., Kruif, K. D., Löhr,
627 F., & Rüterjans, H. (2000). Bovine beta-lactoglobulin: Interaction studies with
628 palmitic acid. *Protein Science, 9*(7), 1347-1356.
629 Renard, D., Lefebvre, J., Griffin, M. C. A., & Griffin, W. G. (1998). Effects of pH and salt
630 environment on the association of beta-lactoglobulin revealed by intrinsic fluorescence
631 studies. *International Journal of Biological Macromolecules, 22*(1), 41-49.
632 Ron, N., Zimet, P., Bargarum, J., & Livney, Y. (2010). Beta-lactoglobulin–polysaccharide
633 complexes as nanovehicles for hydrophobic nutraceuticals in non-fat foods and clear
634 beverages. *International Dairy Journal, 20*(10), 686-693.
635 Russo, G. L. (2009). Dietary n-6 and n-3 polyunsaturated fatty acids: from biochemistry to
636 clinical implications in cardiovascular prevention. *Biochemical Pharmacology, 77*(6),
637 937-946.
638 Sawyer, L., & Kontopidis, G. (2000). The core lipocalin, bovine beta-lactoglobulin.
639 *Biochimica et Biophysica Acta (BBA)-Protein Structure and Molecular Enzymology,*
640 *1482*(1-2), 136-148.
641 Schmitt, C., Bovay, C., Vuilliomenet, A. M., Rouvet, M., Bovetto, L., Barbar, R., & Sanchez,
642 C. (2009). Multiscale characterization of individualized beta-lactoglobulin microgels
643 formed upon heat treatment under narrow pH range conditions. *Langmuir, 25*(14),
644 7899-7909.
645 Shpigelman, A., Israeli, G., & Livney, Y. D. (2010). Thermally-induced protein-polyphenol
646 co-assemblies: beta lactoglobulin-based nanocomplexes as protective nanovehicles for
647 EGCG. *Food Hydrocolloids, 24*(8), 735-743.
648 Singh, H., Ye, A., & Horne, D. (2009). Structuring food emulsions in the gastrointestinal tract
649 to modify lipid digestion. *Progress in Lipid Research, 48*(2), 92-100.
650 Spector, A. A., & Fletcher, J. E. (1970). Binding of long chain fatty acids to beta-
651 lactoglobulin. *Lipids, 5*(4), 403-411.
652 Wang, Q. W. Q., Allen, J. C., & Swaisgood, H. E. (1998). Protein concentration dependence
653 of palmitate binding to beta-lactoglobulin. *Journal of Dairy Science, 81*(1), 76-81.
654 Wu, S. Y., Pérez, M. D., Puyol, P., & Sawyer, L. (1999). Beta-Lactoglobulin binds palmitate
655 within its central cavity. *Journal of Biological Chemistry, 274*(1), 170-174.
656 Yang, M. C., Chen, N. C., Chen, C. J., Wu, C. Y., & Mao, S. J. T. (2009). Evidence for beta-
657 lactoglobulin involvement in vitamin D transport in vivo-Role of the γ-turn (Leu-Pro-
658 Met) of beta-lactoglobulin in vitamin D binding. *FEBS Journal, 276*(8), 2251-2265.
659 Yang, M. C., Guan, H. H., Liu, M. Y., Lin, Y. H., Yang, J. M., Chen, W. L., Chen, C. J., &
660 Mao, S. J. T. (2008). Crystal structure of a secondary vitamin D3 binding site of milk
661 beta-lactoglobulin. *Proteins: Structure, Function, and Bioinformatics, 71*(3), 1197-
662 1210.
663 Zhao, G., Etherton, T. D., Martin, K. R., Vanden Heuvel, J. P., Gillies, P. J., West, S. G., &
664 Kris-Etherton, P. M. (2005). Anti-inflammatory effects of polyunsaturated fatty acids
665 in THP-1 cells. *Biochemical and Biophysical Research Communications, 336*(3), 909-
666 917.

667   Zock, P. L., & Katan, M. B. (1998). Linoleic acid intake and cancer risk: A review and meta-
668   analysis. *American Journal of Clinical Nutrition, 68*(1), 142-153.
669
670

671   Table 1: Binding constants of linoleate/βlg with different forms of βlg determined by ITC and fluorescence. For ITC, association constant K_a

672   and molar ratio n of linoleate/βlg were derived using a "two set of binding sites" model. For fluorescence, two methods of fitting were used.

673   Association constants K_a and molar ratio n of linoleate/βlg were determined using a modified Scatchard method. Experiments with linoleate

674   binding to βlg nanoparticles could not be fitted using modified Scatchard method (non applicable, NA). Sequential linear regression ($L_{total} = f(F \times$

675      $P_{total})$) model was used to determine n. n_1 K_{a1} and n_2 K_{a2} were the binding constant for the first and second binding sites, respectively. Results

676   represent mean ± SD (n=3). K_{a1} and K_{a2}, and n_1 and n_2 of the same complex were significantly different, independently of the method and the βlg

677   form used, with P-value inferior to 0.01 and to 0.05, respectively; except for K_{a1} and K_{a2} data obtained with the modified Scatchard of the

678   linoleate/native βlg complex (*).

679

680

	ITC			Fluorescence: Modified Scatchad			Fluorescence: $L_{total} = f(F \times P_{total})$		
	Linoleate/ native βlg	Linoleate/ dimers	Linoleate/ nanoparticles	Linoleate/ native βlg	Linoleate/ dimers	Linoleate/ nanoparticles	Linoleate/ native βlg	Linoleate/ dimers	Linoleate/ nanoparticles
n_1	0.60 ± 0.01	0.53 ± 0.08	0.92 ± 0.29	2.45 ± 0.07	10.31 ± 0.05	NA	2.38 ± 0.12	9.8 ± 0.21	15.74 ± 0.55
$K_{a1} \times 10^5$ M^{-1}	17.95 ± 6.29	15.13 ± 9.53	15.83 ± 3.35	9.20 ± 2.65*	14.67 ± 2.12				
n_2	6.79 ± 0.05	8.64 ± 0.54	10.25 ± 1.65	5.27 ± 1.50	15.29 ± 0.71		6.02 ± 0.29	12.54 ± 0.76	40.73 ± 2.17
$K_{a2} \times 10^5$ M^{-1}	0.41 ± 0.05	0.50 ± 0.42	0.57 ± 0.22	0.62 ± 0.49*	0.37 ± 0.13				

681   Table 2: Protein proportion of linoleate/βlg complexes with different forms of βlg (native,

682   covalent dimers and nanoparticles), obtained by GP-HPLC. 0, 5, 7.5 and 10 represents the

683   initial molar ratios of linoleate/βlg. βlg M, βlg monomers; βlg D, βlg dimers; βlg O, βlg

684   oligomers; NanoP, βlg nanopaticles. Results represent mean ± SD (n=3).

685

Initial linoleate/βlg		0			5			7.5			10		
Linoleate/ native βlg	βlg M	88.45	±	5.24	66.44	±	8.24	60.43	±	8.17	51.09	±	4.95
	βlg D	6.64	±	2.63	23.13	±	6.94	28.22	±	9.57	34.94	±	6.78
	βlg O	4.92	±	2.78	10.43	±	4.51	11.35	±	2.03	13.97	±	3.97
Linoleate/ dimer	βlg M	16.29	±	1.50	14.43	±	0.50	14.05	±	0.19	13.39	±	0.61
	βlg D	78.27	±	3.21	78.62	±	4.23	79.55	±	5.80	77.88	±	6.48
	βlg O	5.43	±	1.65	6.95	±	2.70	6.41	±	3.74	8.72	±	4.22
Linoleate/ nanoparticle	βlg M	22.41	±	1.36	15.82	±	2.48	11.96	±	1.03	10.65	±	1.95
	NanoP	77.59	±	1.36	84.18	±	2.48	88.04	±	1.03	89.35	±	1.95

686

687   *FIGURES*

688

689   Figure 1: Binding association of linoleate/βlg with different forms of βlg obtained by ITC

690   and fluorescence. (A) For the ITC experiments, linoleate was titrated in different forms of βlg

691   (native, covalent dimers and nanoparticles) in PBS buffer (pH 7.4) at 25°C. βlg (0.027 µM)

692   were titrated with increments of 10 µL linoleate (1.65 µM). Results represent the integrated

693   raw heat signals plotted against the linoleate/βlg molar ratio. (B) For the intrinsic fluorescence

694   experiments, linoleate (5mM) was titrated in 10 µM βlg (native, covalent dimers and

695   nanoparticles) at 25°C. Results represent the fluorescence at 345 nm corrected by the blank

696   (NATA). ─○─, linoleate /native βlg; --✕--, linoleate/covalent dimers; --●--, linoleate

697   /nanoparticles. Results represent mean ± SD (n=3).

698

699   Figure 2: SDS-PAGE profiles of the three linoleate/βlg complexes. Non-reducing

700   conditions were used for: (A) linoleate/native βlg complexes, (B) linoleate/covalent dimers

701   complexes, and (C) linoleate/nanoparticles complexes. Reducing conditions were used for the

702   gel (D) corresponding to the profile of linoleate/nanoparticles βlg complexes (similar profiles

703   were obtained for the two other complexes). M_w, molecular weight markers (14.4, 20.1, 30,

704   45, 66, 97 kDa); βlg, βlg control; lanes 5, 7.5 and 10, complexes with an initial molar ratio of

705   5, 7.5 and 10 linoleate/βlg, respectively.

706

707   Figure 3: Stoichiometry of linoleate/βlg with different forms of βlg (native, covalent

708   dimers and nanoparticles) as determined by GC after dialysis. Correlation of the molar ratios

709   of linoleate/βlg added to the starting solutions with the molar ratios of linoleate/βlg that were

710   detected by GC analysis in the linoleate/βlg samples after extensive dialysis and freeze-

711   drying. ─○─, linoleate /native βlg; --✕--, linoleate/covalent dimers; --●--, linoleate

712   /nanoparticles.

713

714   Figure 4: Cytotoxicity of linoleate, free or bound to different forms of βlg, using Caco-2

715   cells. Cell viability after 24 h on 2×10^4 Caco-2 cells compared to control cells was assessed

716   using an MTS assay. Linoleate concentrations in the tested sample varied from 0 to 200 µM.
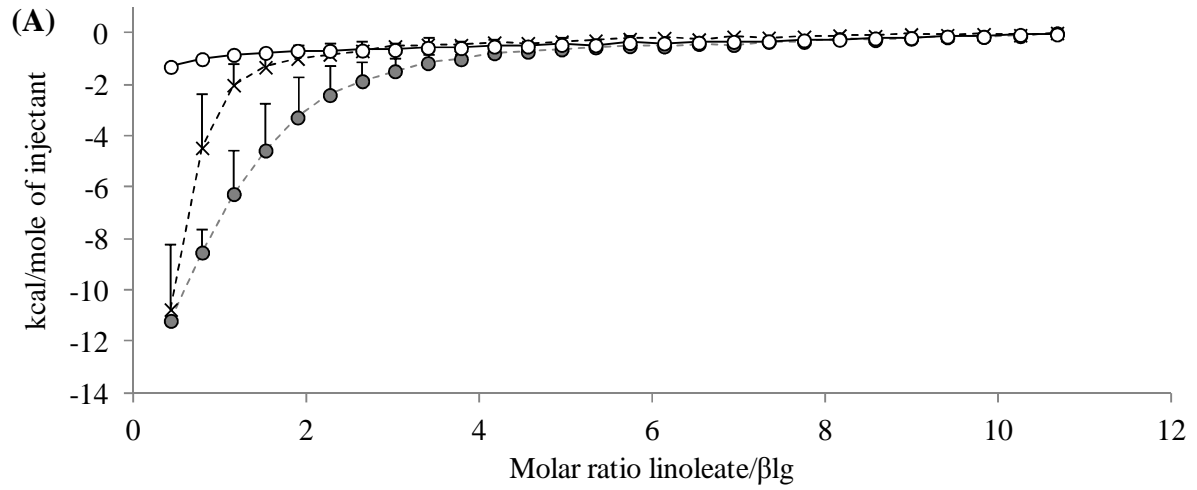
717   ─■─, free linoleate; ─○─, linoleate /native βlg; --✕--, linoleate/covalent dimers; --●--,

718   linoleate /nanoparticles.

Figure 1

721   —○—Linoleate/native βlg   --✗-- Linoleate/dimers   --●-- Linoleate/nanoparticles

722
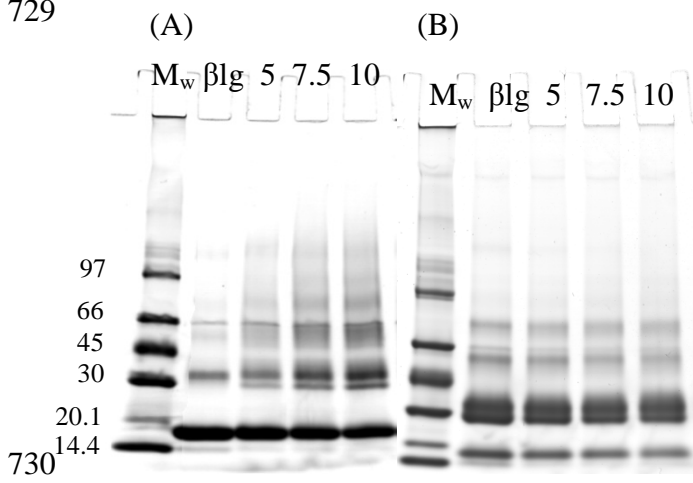

723
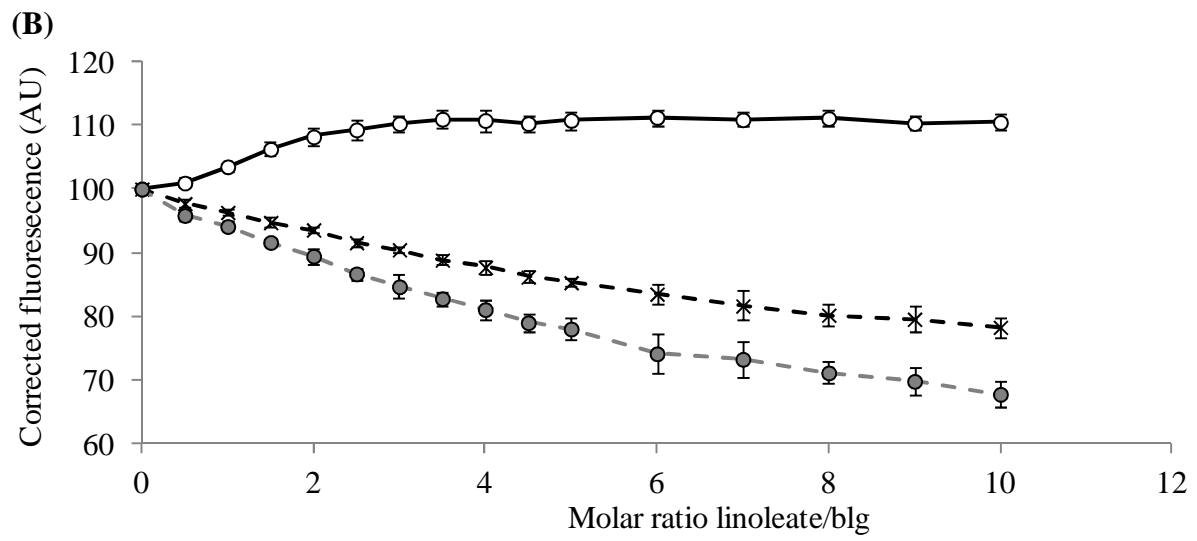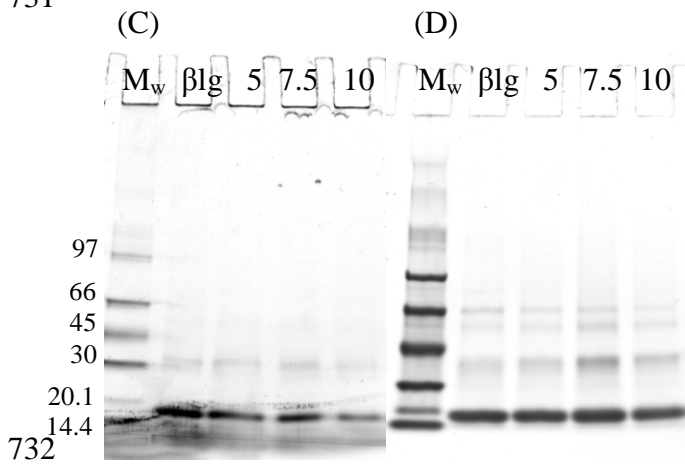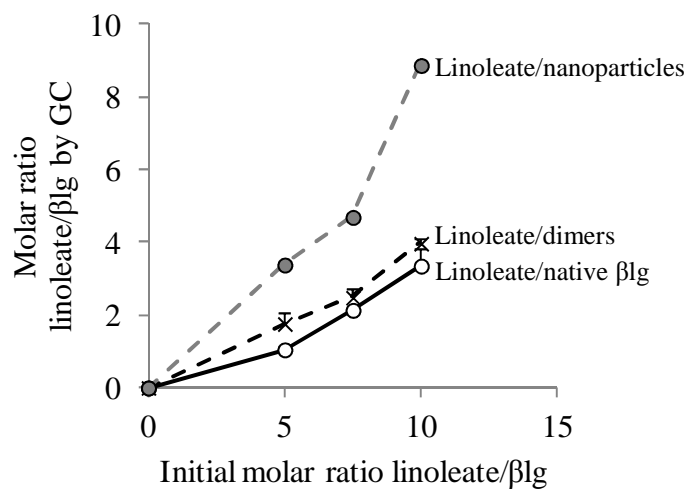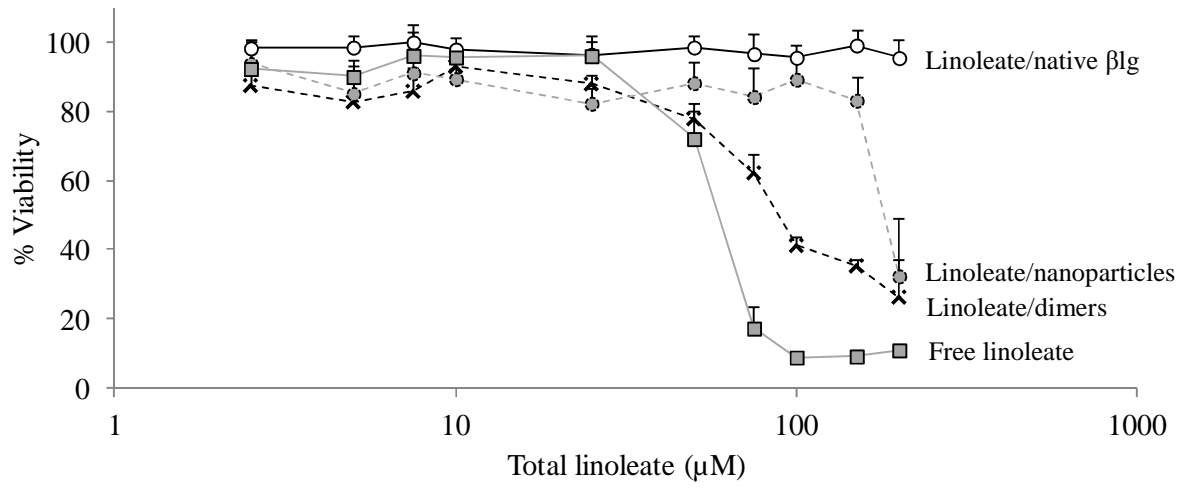

724

725

726

727   Figure 2

728

729

733   Figure 3

734

735   Figure 4

736

737

738